

ac susceptibility of $\text{Sr}_3\text{CuPt}_x\text{Ir}_{1-x}\text{O}_6$: A magnetic system with competing interactions and dimensionality

S. H. Irons, T. D. Sangrey, and K. M. Beauchamp

Department of Physics, Wesleyan University, 265 Church Street, Middletown, Connecticut 06457

M. D. Smith and H.-C. zur Loye

Department of Chemistry and Biochemistry, University of South Carolina, Columbia, South Carolina 29208

(Received 2 December 1999)

$\text{Sr}_3\text{CuPt}_x\text{Ir}_{1-x}\text{O}_6$ has been cited as an example of a one-dimensional quantum spin chain with competing ferromagnetic and antiferromagnetic interactions. We have measured the ac susceptibility of $\text{Sr}_3\text{CuPt}_x\text{Ir}_{1-x}\text{O}_6$ with $x=0, 0.1, 0.2, 0.3, 0.4, 0.5, 0.6,$ and 0.7 , in magnetic fields of 0–60 kOe, and at temperatures down to 0.275 K. Our data show that the $x=0$ endpoint, $\text{Sr}_3\text{CuIrO}_6$, exhibits long-range ferromagnetic order at $T=20.1$ K, contrary to results from dc susceptibility studies which indicated that it remained a one-dimensional ferromagnet to below 4 K. When platinum is substituted for iridium, antiferromagnetic couplings are introduced, and the susceptibility shows a diminishing signature of the three-dimensional ferromagnetic transition. Furthermore, the low-temperature susceptibility exhibits peaks which appear and evolve as x is increased. These results lead to a rich phase diagram in temperature and Pt concentration space. We find that the behavior of $\text{Sr}_3\text{CuPt}_x\text{Ir}_{1-x}\text{O}_6$ cannot be simply described by the random quantum spin chain theories that were developed, in part, to address this system.

I. INTRODUCTION

Materials that exhibit low-dimensional magnetic properties are fascinating systems from both a theoretical and experimental standpoint. In one-dimensional systems both quantum and thermal fluctuations dominate ordering interactions, giving rise to unique ground states and excitation spectra.¹ Since calculations are simplified in one dimension, many exact results as well as numerical calculations are available.² For these reasons, a number of magnetic materials that possess a linear magnetic structure have been studied.¹ In particular, an interesting series of isostructural, one-dimensional oxides, which exhibit a range of magnetic behavior, has recently been investigated. These materials are of the type $A_3A'BO_6$, and are structurally similar to the compounds $A_4\text{PtO}_6$, where $A=\text{Sr}, \text{Ca}, \text{Ba}$.³ The $A_3A'BO_6$ compounds consist of chains of alternating, face sharing $A'O_6$ trigonal prisms and BO_6 octahedra, which form a triangular lattice separated by A^{2+} ions (see Fig. 1). Compounds of this type have been synthesized with a large variety of elements in various oxidation states, including $A'=\text{Ni}^{2+}, \text{Cu}^{2+},$ and Zn^{2+} , $B=\text{Pt}^{4+}, \text{Ir}^{4+},$ and Rh^{4+} , and $A'=B=\text{Co}$, with an unknown valence.^{4–6} The magnetic susceptibility of these materials has been fitted to a variety of models, including that of the Ising antiferromagnetic chain ($\text{Sr}_3\text{ZnIrO}_6$) and that of noninteracting ions with large single ion anisotropy ($\text{Sr}_3\text{NiPtO}_6$).^{7,8} Ferrimagnetic coupling of ferromagnetic chains has been postulated for $\text{Ca}_3\text{Co}_2\text{O}_6$.⁶ The Heisenberg antiferromagnetic chain model has been applied to $\text{Sr}_3\text{CuPtO}_6$, and ferromagnetic interactions have been observed in $\text{Sr}_3\text{CuIrO}_6$.^{4,8}

By making solid solutions of $\text{Sr}_3\text{CuPtO}_6$ and $\text{Sr}_3\text{CuIrO}_6$, a series of spin chain materials with both ferromagnetic and antiferromagnetic interactions can be formed.⁹ The resulting

compounds, $\text{Sr}_3\text{CuPt}_x\text{Ir}_{1-x}\text{O}_6$, have random ferromagnetic and antiferromagnetic bonds, with segments of one interaction sign with lengths that vary with x . Cu^{2+} and Ir^{4+} , both $S=1/2$ ions, interact ferromagnetically, as in $\text{Sr}_3\text{CuIrO}_6$. The Cu^{2+} ions interact antiferromagnetically in a Cu-Pt-Cu segment, where Pt^{4+} has $S=0$, as in $\text{Sr}_3\text{CuPtO}_6$. The replacement of one Pt ion in $\text{Sr}_3\text{CuPtO}_6$ with one Ir ion replaces a single antiferromagnetic bond with two ferromagnetic bonds. The random quantum spin chain (RQS) theory^{10–14} was developed to apply to chains of Heisenberg spins with a mixture of antiferromagnetic and ferromagnetic interactions. This theory identifies three distinct regimes for spin interactions. At high temperatures all spins are uncorrelated and Curie-like; at intermediate temperatures ($k_bT \sim J$) they correlate within segments but the segments remain independent from each other; and at low temperatures, intersegment correlations become significant. The dc susceptibility of $\text{Sr}_3\text{CuPt}_x\text{Ir}_{1-x}\text{O}_6$ compounds with $x=0, 0.25, 0.5, 0.75,$ and 1 was measured at a field of 5 kOe, and was found to agree qualitatively with the predictions of the RQS theory.⁹

In order to probe the relevance of the RQS theory to this series of compounds more deeply, it is important to measure the magnetic susceptibility in a small magnetic field, and down to as low a temperature as possible. In particular, for materials where there are ferromagnetic interactions, an applied magnetic field suppresses the susceptibility from its zero-field value and precludes a comparison with theoretical models. We have measured the ac susceptibility of powders of the solid solution $\text{Sr}_3\text{CuPt}_x\text{Ir}_{1-x}\text{O}_6$ with $x=0, 0.1, 0.2, 0.3, 0.4, 0.5, 0.6,$ and 0.7 in applied magnetic fields from 0–60 kOe, down to temperatures of 0.275 K. In measuring ac susceptibility in the zero-field limit, we have found deviations from the RQS model, primarily arising from strong ferromagnetic interactions. We find that $\text{Sr}_3\text{CuIrO}_6$ undergoes a transition to long-range ferromagnetic order at $T_c=20.1$ K, and that this transition is suppressed, but not re-

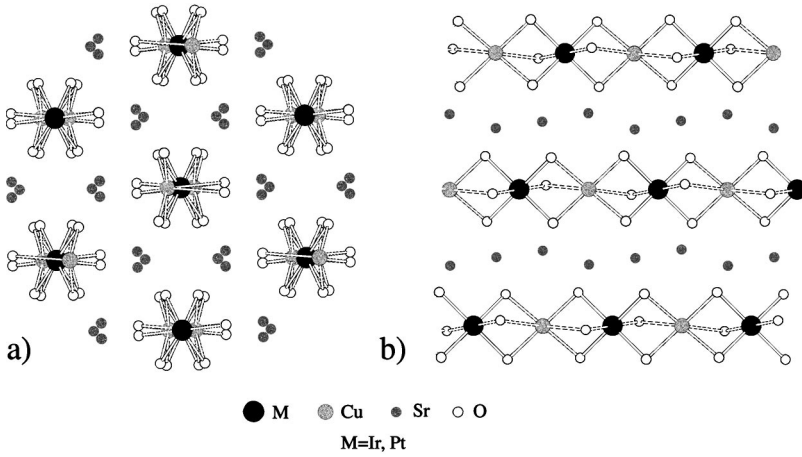


FIG. 1. Crystal structure of Sr_3CuMO_6 ($M = \text{Ir, Pt}$). (a) Looking down on the chains. The chains form a triangular lattice separated by Sr^{2+} ions. The Cu^{2+} ions move to the left or right going down the chains. (b) Looking along three the chains in the center of part (a). The chains consists of alternating, face sharing CuO_6 trigonal prisms and MO_6 octahedra. The Cu^{2+} ions move into and out of the figure plane, so from this perspective they look colinear with the Ir^{4+} ions.

moved by application of a magnetic field. In addition, for $x > 0$ we find low-temperature peaks in the susceptibility that evolve to lower temperatures as x is increased. We present here detailed measurements of the magnetic susceptibility of $\text{Sr}_3\text{CuPt}_x\text{Ir}_{1-x}\text{O}_6$ as a function of x , temperature, and magnetic field.

II. EXPERIMENTAL DETAILS

Powders of $\text{Sr}_3\text{CuPt}_x\text{Ir}_{1-x}\text{O}_6$ were prepared via solid-state reactions, using stoichiometric amounts of starting materials, as described elsewhere.^{4,9} In this paper we present results for $x = 0, 0.1, 0.2, 0.3, 0.4, 0.5, 0.6,$ and 0.7 . Three $x = 0.5$ samples, synthesized at different times, were measured, and all gave the same results. X-ray-diffraction data indicate that the micron sized crystallites that make up the powders are single phase. The powders were pressed into cylindrical pellets (diameter = 0.29 cm) at least 0.76 cm long so as to maximize the signal from the ac susceptometer. After pressing, they were individually sintered in air at 1150°C for 4–14 h in clean alumina boats. Their post-sintered density ranged from 70 to 86% of the theoretical value of 6.74 g/cm^3 . The demagnetization factors of the samples are less than 0.113.

dc magnetization measurements were taken in a Quantum Design superconducting quantum interference device susceptometer at temperatures from 2 to 300 K, and susceptibility was calculated by dividing by the applied field. ac susceptibility was measured at temperatures from 0.275 to 30 K using a differential coil susceptometer mounted in an Oxford He^3 cryostat. The samples were placed within one coil of a pair of oppositely wound secondary coils balanced to give a near null signal when empty. The primaries, which were 2.4 times longer than the secondaries to reduce finite solenoid effects, provided an rms field of $5\text{--}25 \times 10^{-3} \text{ Oe}$. The data were taken using a computer-controlled EG&G lock-in amplifier at frequencies between 53 and 6011 Hz. We measured $\chi = \chi' + i\chi''$, where χ' is the real part of the susceptibility (90° out of phase with the primary signal), and χ'' is the imaginary part of the susceptibility (in phase with the primary signal). It is important to note, that since we are measuring the susceptibility of a powder, if the spin dimensionality is not isotropic, the signal will include transverse as well as longitudinal components of the susceptibility.

The sample was thermally grounded through a sapphire

rod to the He^3 reservoir. The susceptometer was calibrated against the known low-temperature susceptibility of Yb_2O_3 as well as the diamagnetic signal of a cylinder of superconducting aluminum. In addition, the ac susceptibility was matched to the dc susceptibility in the paramagnetic regime. Demagnetization corrections had very little effect on the magnitude of the susceptibility. The susceptibility is reported in units of ($\text{cm}^3/\text{mol spin}$), since the number of spins per unit cell changes from 2 to 1 as x is increased from 0 to 1.

III. RESULTS AND DISCUSSION

The crystal structure of Sr_3CuMO_6 ($M = \text{Pt, Ir}$) has a monoclinic space group $C2/c$. Figure 1 shows the crystal structure (a) looking down the chains and (b) looking at the chains from the side. The one-dimensional structure of Sr_3CuMO_6 is not that of a simple linear chain. The M^{4+} ions lie in a straight line, separated by a distance of $d_{M-M}^{\text{intrachain}} = 5.63 \text{ \AA}$. The Cu^{2+} ions, however, are offset from the chain axis toward one of the faces of the oxygen trigonal prism by 0.53 \AA [shown in Fig. 1 (a)], in order to maintain a pseudosquare planar coordination. The direction of the offset rotates by 180° from one Cu^{2+} ion to the next along the chain. The in-chain $\text{Cu}-M$ distance $d_{\text{Cu}-M}^{\text{intrachain}} = 2.86 \text{ \AA}$. Each chain has six nearest-neighbor chains, and the distance between the chain axes is $d_{\text{axis}} = 5.53 \text{ \AA}$. The chains are separated from one another by Sr^{2+} ions. The M^{4+} ions along the chain are offset from those on neighboring chains by $(1/3)d_{M-M}^{\text{intrachain}}$ [shown in Fig. 1(b)], making the closest interchain $M-M$ distance $d_{M-M}^{\text{interchain}} = 5.83 \text{ \AA}$. Because of the distortion of the Cu^{2+} ion away from the chain axis, any single Cu^{2+} ion has two nearest-neighbor Cu^{2+} ions in neighboring chains, at a distance of $d_{\text{Cu}-\text{Cu}}^{\text{interchain}} = 5.09 \text{ \AA}$ and two nearest-neighbor M^{4+} ions in neighboring chains at a distance of $d_{\text{Cu}-M}^{\text{interchain}} = 5.24 \text{ \AA}$. The next-nearest interchain $\text{Cu}-\text{Cu}$ distance is $d_{\text{Cu}-\text{Cu}}^{\text{interchain}}(2) = 5.92 \text{ \AA}$ and the $\text{Cu}-M$ distance is $d_{\text{Cu}-M}^{\text{interchain}}(2) = 5.64 \text{ \AA}$. The nearest $\text{Cu}-\text{Cu}$ and $\text{Cu}-M$ interchain distances are not uniformly distributed either along the chains or between the chains, and no flat plane of second nearest neighbors exists. The spins are believed to interact along the chains through superexchange mediated by the oxygen ions. Despite this complexity in the chain structure, Sr_3CuMO_6 are nevertheless structurally highly one-dimensional materials. $\text{Sr}_3\text{CuIrO}_6$ has an intrachain mag-

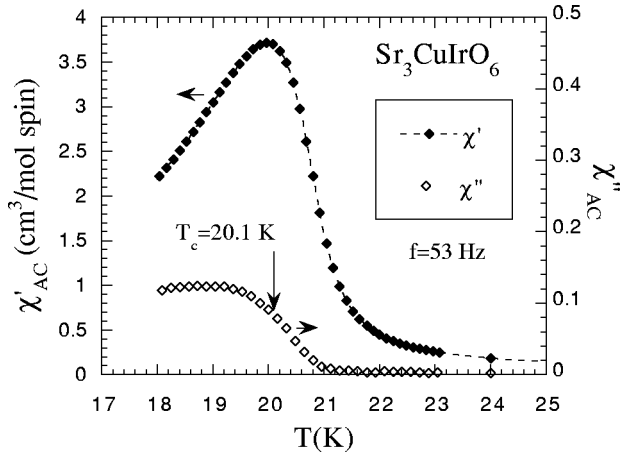


FIG. 2. χ' and χ'' vs temperature for $\text{Sr}_3\text{CuIrO}_6$ at 53 Hz.

netic ion distance of 2.86 Å and an interchain magnetic ion distance of 5.09 Å. The isostructural $\text{Sr}_3\text{CuPtO}_6$ is less one-dimensional, with an intrachain Cu-Cu distance of 5.72 Å, and an interchain Cu-Cu distance of 5.09 Å. However, the magnetic dimensionality is determined by the strength of the magnetic couplings, not strictly by the distances between the ions.

A. $\text{Sr}_3\text{CuPtO}_6$

Initial measurements of the dc susceptibility of powdered $\text{Sr}_3\text{CuPtO}_6$ ($x=1$) gave a Curie-Weiss temperature of $\theta = zJ/4k_B = -47$ K with a g factor of 1.99.¹⁵ The dc susceptibility of single crystalline $\text{Sr}_3\text{CuPtO}_6$ was also measured down to 2 K in a magnetic field of 5 kOe.⁸ The data were well fit to a one-dimensional Heisenberg antiferromagnetic model with interchain interactions. The fit gave an intrachain interaction energy of $J/k_B = -49.4$ K, and an interchain interaction energy $zJ' = -29.2$ K. (Note that the J values reported here are twice the values reported in the reference. This is because the Hamiltonian on which the fit is based takes $2J$ as the spin-spin interaction energy, whereas we take the spin-spin interaction energy as J .) The only other measurement of this compound that we know of is electron spin resonance (ESR), carried out on $\text{Sr}_3\text{CuPtO}_6$ powder.¹⁶ This study finds a slightly anisotropic, temperature independent g factor. We do not present ac susceptibility for $\text{Sr}_3\text{CuPtO}_6$, since its susceptibility is field independent and we find no significant difference between the ac and dc susceptibilities. We also find no signature of three-dimensional ordering down to $T=0.27$ K.

B. $\text{Sr}_3\text{CuIrO}_6$

The dc susceptibility of $\text{Sr}_3\text{CuIrO}_6$ in the paramagnetic region follows two different Curie-Weiss Laws. For temperatures of $230 < T < 300$ K, the Curie-Weiss temperature $\theta = zJ/4k_B = -16$ K and the Landé g factor is $g=1.9$. For $100 < T < 200$ K, $\theta=40$ K and $g=1.7$. The lower temperature Curie constant indicates that the dominant interaction at temperatures below 200 K is ferromagnetic. A peak is observed in the real part of the ac susceptibility χ'_{AC} at $T_c = 20.1$ K, as shown in Fig. 2. We identify this peak as the transition point to long-range order which has a significant

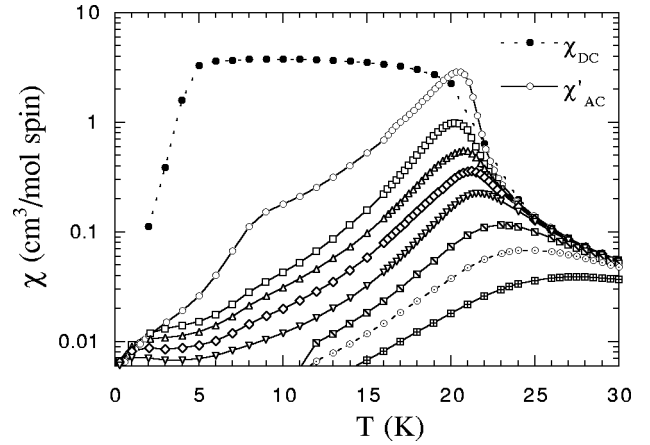


FIG. 3. Log plot of χ vs temperature for $\text{Sr}_3\text{CuIrO}_6$. The filled symbols show χ_{DC} at an applied field of 0.25 kOe. The open symbols show χ'_{AC} at applied fields of $H=0, 0.1, 0.25, 0.5, 1, 2.5, 5,$ and 10 kOe. The peak at 20 K is steadily suppressed and moves up in temperature which is consistent with long-range ferromagnetic ordering.

ferromagnetic character. This transition temperature is about half of the mean-field Weiss temperature. χ'' rises at 21 K and levels off by 19.5 K, reflecting dissipation at the transition, primarily due to domain-wall motion. A difference between zero field cooled (ZFC) and field cooled (FC) susceptibility appears at $T=20.8$ K, indicating that there is an irreversibility even above T_c , possibly due to domain-wall pinning on the small crystallite boundaries. The susceptibility does not diverge below 20.9 K, but rolls over to a rounded peak. It is possible that the transition is not to a pure ferromagnet, but may be to a canted ferromagnet or some other more complicated magnetic order.

Using $T_c = 20.1$ K, we looked for critical exponents in the susceptibility. We found that the best fit to $\ln \chi$ vs $\ln(t)$, where $t = (T - T_c)/T_c$, gives a straight line with a slope of 1.75, but only over a very limited temperature range: $20.9 < T < 21.7$ K ($0.041 < t < 0.09$). A slope of 1.75 corresponds to the two-dimensional Ising model.¹⁷ It seems reasonable that the spins could be Ising-like, since the isostructural $\text{Sr}_3\text{ZnIrO}_6$ orders as a one-dimensional Ising antiferromagnet.⁷ However, the crystal structure does not suggest an obvious plane in which two-dimensional ordering could occur. Nevertheless, $\text{Sr}_3\text{CuIrO}_6$ develops long-range (presumably three-dimensional) order at 20.1 K, and shows no signature of one-dimensional magnetism.

Figure 3 compares the dc and ac susceptibilities measured for a range of magnetic fields. χ_{DC} was measured at 0.25 kOe. χ'_{AC} was measured at applied fields of 0, 0.1, 0.25, 0.5, 1, 2.5, 5.0, and 10 kOe. χ'_{AC} ($H=0$) is larger than χ_{DC} ($H=0.25$ kOe) just above the transition, where ferromagnetic fluctuations are suppressed by the 0.25-kOe dc field, but is lower than χ_{DC} ($H=0.25$ kOe) below the transition, where domain-wall pinning prevents the spins from responding to the ac field. χ'_{AC} is monotonically suppressed and the peak is moved to higher temperature by the applied magnetic field, as is expected for a ferromagnet. There is no evidence for a field induced transition to one-dimensional magnetism.

A shoulder is evident in the zero field χ'_{AC} at $T=9$ K. This shoulder is suppressed more rapidly in an applied field

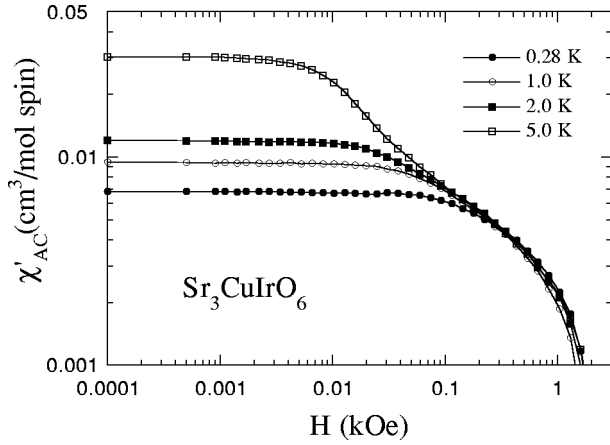


FIG. 4. Log zero-field-cooled χ'_{AC} vs log applied field of $\text{Sr}_3\text{CuIrO}_6$ at low temperatures.

than the overall signal. A small, but discernible, peak is found in χ''_{AC} at $T=9$ K, indicating that the shoulder in χ'_{AC} could be due to a phase transition. At a slightly lower temperature, χ_{DC} drops rapidly to zero, indicating a change from a ferromagnetically aligned state to a state with a small or zero spontaneous moment. This state could be a ferromagnetic domain state, or either a ferrimagnetic or an antiferromagnetic state. The field dependence is also suppressed at the lowest temperatures, as can be seen in Fig. 3 by the coincidence of the low temperature tails of χ'_{AC} at different fields.

To further explore the field dependence of the low-temperature phase, we measured magnetic-field dependence of the ZFC susceptibility at temperatures below 5 K, shown in Fig. 4. At the lowest temperature ($T=0.275$ K) the susceptibility is field independent up to 1 kOe. This behavior corresponds to a linearly increasing magnetization as a function of field caused either by domain-wall motion or spin reorientation. As the temperature is increased from $T=0.275$ K, the susceptibility increases, but the field to which the susceptibility remains field independent decreases. At $T=5$ K, the susceptibility is field independent only up to 40 Oe. The field dependence of the susceptibility is the same for all temperatures at fields above $H=1$ kOe. At a field of about 20 kOe, the susceptibility drops sharply as the magnetization approaches saturation. No peaks are found in the field dependence of the susceptibility, which indicates that no phase transitions are traversed by applying a magnetic field.

The magnetization was previously measured at 5 K in fields up to 200 kOe, and was found to reach $0.5 \mu_B/\text{mol}$ at an applied field near 1 kOe and to only increase slowly to $0.7 \mu_B/\text{mol}$ up to 200 kOe.⁴ A saturation magnetization of $0.7 \mu_B/\text{mol}$ is much smaller than the expected $2 \mu_B/\text{mol}$ for the two spins per unit cell found in $\text{Sr}_3\text{CuIrO}_6$. The low-temperature phase, then, could be a canted antiferromagnet. The applied field increases the canting, but does not cause a spin reorientation transition. Since the applied field will only cause canting in one of the three crystalline directions, the powder magnetization should only show 1/3 of the expected saturation magnetization. For two spins, then, we would expect the saturation magnetization to be $2/3 \mu_B/\text{mol}$, very

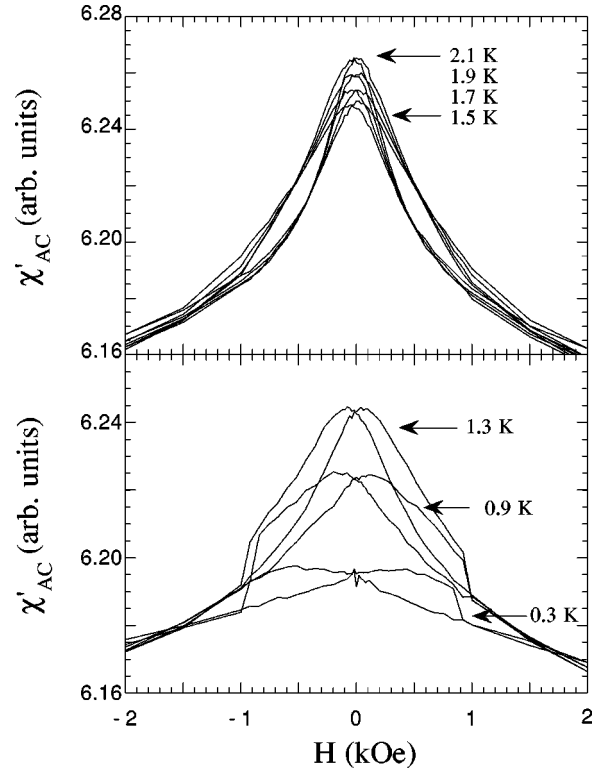


FIG. 5. Hysteresis curves for $\text{Sr}_3\text{CuIrO}_6$ at low temperatures, showing the Barkhausen effect at the lowest temperatures. Integration to obtain magnetization results in loops with extremely small areas.

close to the measured value. Kageyama *et al.* explain similar results found in $\text{Ca}_3\text{Co}_2\text{O}_6$ as ferrimagnetic ordering of ferromagnetic chains.⁶

By measuring hysteresis loops in χ'_{AC} , shown in Fig. 5, we can map out regions of reversible and irreversible behavior. Hysteresis is observed at all temperatures below the transition temperature of 20.1 K, and it changes in character as the temperature decreased. The two peaks symmetric about $H=0$ correspond to a small, but finite, area enclosed in the magnetization loop and indicate that domain-wall motion is irreversible. At temperatures below 1.5 K, the ac susceptibility displays a sharp jump near $H=1$ kOe. This jump is a signature of the Barkhausen effect, which occurs when ferromagnetic domains suddenly and irreversibly reorient themselves in response to the applied field.¹⁸ The fact that the jumps always occur at approximately the same field, indicate a fairly narrow distribution of domain-wall pinning energies. This behavior is consistent with a low-temperature phase ($T < 5$ K) which has a ferromagnetic component, like a canted antiferromagnet or a ferrimagnet, and an intermediate temperature phase ($5 < T < 20$ K) which is a more generic ferromagnet of undetermined structure.

C. $\text{Sr}_3\text{CuPt}_x\text{Ir}_{1-x}\text{O}_6$

As Pt is doped in place of Ir in $\text{Sr}_3\text{CuIrO}_6$, the ferromagnetic character of the compounds decreases and the antiferromagnetic character increases. The high-temperature susceptibility of the series of compounds follows Curie-Weiss behavior with a Curie constant that is appropriate for a spin-1/2 system, but with a Curie-Weiss temperature which

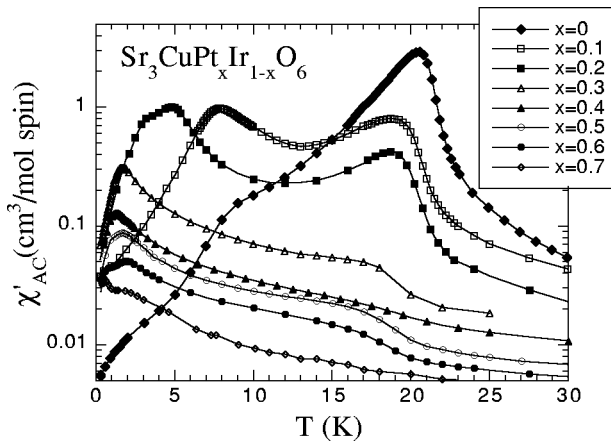


FIG. 6. Log χ'_{AC} vs temperature for different Pt concentrations. As Pt doping is increased the ferromagnetic peak is suppressed and low-temperature peaks and shoulders develop.

changes continuously from the positive value of $\text{Sr}_3\text{CuIrO}_6$ to the negative value of $\text{Sr}_3\text{CuPtO}_6$.⁹ Although the authors do not state this result explicitly, the change in the Curie-Weiss temperature is also seen in the paramagnetic region of the RQS theory.¹⁰ The agreement between the theory and the experiment in the paramagnetic region does not necessarily indicate anything about the dimensionality of the magnetism, but it does indicate that the samples contain a homogeneous mixture of ferromagnetic and antiferromagnetic bonds. Without such a homogeneous mixture, the susceptibility in the paramagnetic region would be dominated by the ferromagnetic interactions, giving a much more slowly changing Curie-Weiss temperature.

In addition to the change in sign of the magnetic interaction, the dimensionality of the interactions must also change from three dimensional to one dimensional, as Pt is doped in place of Ir. Furthermore, although $\text{Sr}_3\text{CuIrO}_6$ orders three dimensionally, we expect that as the temperature is lowered, the correlation length along the ferromagnetic chains (ξ_{chain}^{FM}) grows faster than the correlation length between the chains. Substitution of Pt for Ir limits the extent of ξ_{chain}^{FM} by breaking ferromagnetic bonds. Although Pt is a nonmagnetic ion, the substitution of Pt for Ir creates an antiferromagnetic bond between its two neighboring Cu^{2+} ions. This antiferromagnetic bond effectively decouples the one-dimensional ferromagnetic subsections and limits ξ_{chain}^{FM} to the length of a particular ferromagnetic chain.¹¹ With a 10% substitution of Pt for Ir, the average length of a purely ferromagnetic chain is reduced from infinity to nine spins.¹¹ Limiting the length of ferromagnetic chains should also limit the interactions between those chains, causing an evolution to one-dimensional behavior.

The effect on the ac susceptibility of substituting Pt for Ir can be observed in Fig. 6. The magnitude of the 20-K peak found in $\text{Sr}_3\text{CuIrO}_6$ is strongly suppressed and shifted to slightly lower temperatures as the Pt concentration is increased. Once the percentage of Pt reaches 30%, the peak is reduced sufficiently to appear only as a shoulder, which is still observable at 60% Pt concentration. A phase diagram is constructed in Fig. 7, in which closed circles indicate the temperature of the ferromagnetic peak, and the open circles indicate the temperature of the ferromagnetic shoulder. The

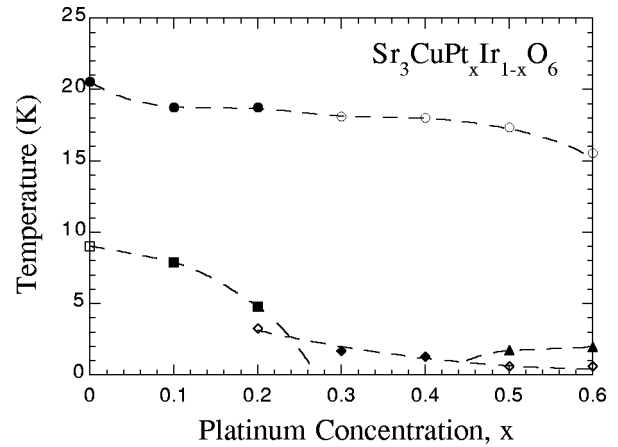


FIG. 7. Peak positions vs platinum concentration. Filled symbols are peaks, open symbols are shoulders. The dotted lines are guides to the eye.

continued existence of the ferromagnetic feature after Pt substitution points to the existence of finite-sized ferromagnetic clusters. The existence of the ferromagnetic clusters is further evidenced by a difference between χ_{DC} and χ'_{AC} up to $x=0.6$. A comparison of χ_{DC} and χ'_{AC} for $x=0.3, 0.5,$ and 0.7 is shown in Fig. 8. The clear difference between χ_{AC} and χ_{DC} at temperatures below T_c for $x=0.3$ and $x=0.5$ indicates that domain-wall pinning is still instrumental in pre-

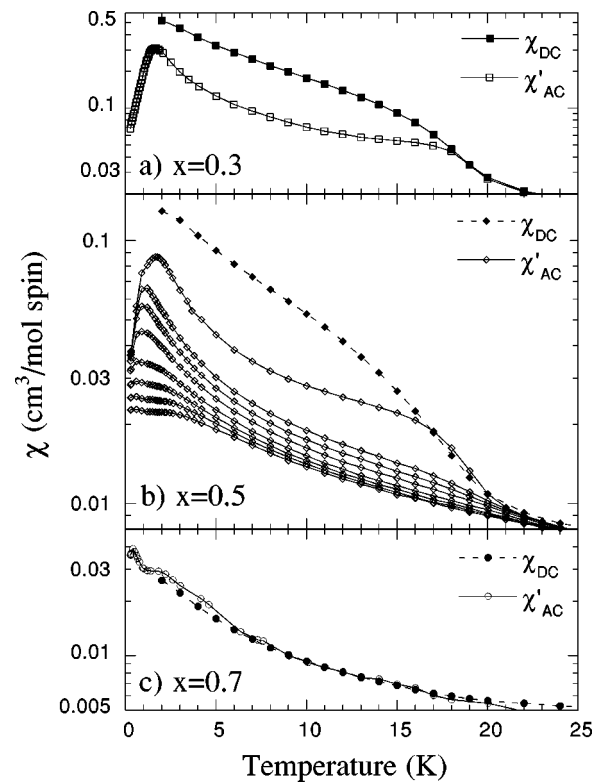


FIG. 8. A comparison of χ'_{AC} in zero applied field (open symbols) and χ_{DC} in an applied field of 0.25 kOe (closed symbols) vs temperature below the $x=0$ ferromagnetic transition temperature. χ_{AC} falls below χ_{DC} in (a) $x=0.3$ and (b) $x=0.5$ where strong ferromagnetic correlations are present, but follows χ_{DC} in (c) $x=0.7$. Also in (b) is χ_{AC} for applied fields of 0.25, 0.5, 1, 2, 3, 4, and 5 kOe.

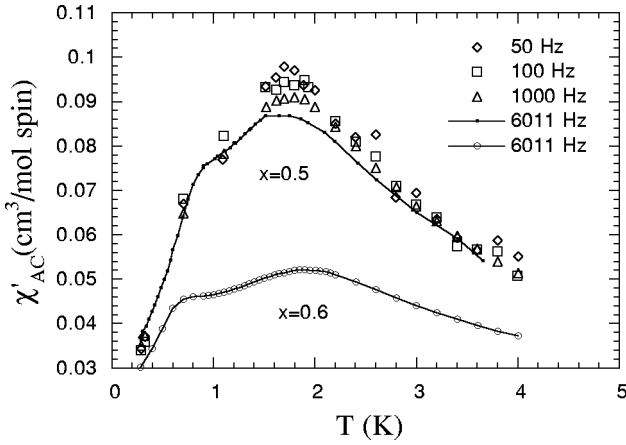


FIG. 9. χ'_{AC} vs temperature for $x=0.5$ and $x=0.6$ showing the evolution of the peak to higher temperatures and the shoulder to lower temperatures. Also shows χ'_{AC} for $x=0.5$ measured at different frequencies.

venting the spins from following the ac field. (The field dependence for $x=0.5$ will be discussed below.) For $x=0.7$, the ac and dc susceptibility are coincident down to 5 K.

In addition to the suppression of the 20-K ferromagnetic peak, two low-temperature features appear as Pt is doped in place of Ir: a low-temperature peak, and a low-temperature shoulder below which the susceptibility drops sharply. These features do not have a clear origin, though their magnitudes and locations do correlate with Pt concentration. By examining the evolution of the peaks with Pt concentration as well as with magnetic field, we construct a tentative low-temperature phase diagram for $\text{Sr}_3\text{CuPt}_x\text{Ir}_{1-x}\text{O}_6$, also shown in Fig. 7. The peaks that occur for $x=0.1$ and $x=0.2$ at $T=8$ K and $T=5$ K, respectively, may be an enhancement of the shoulder seen in χ'_{AC} at $T=9$ K for $x=0$. The peaks for both $x=0.1$ and $x=0.2$ are suppressed and move to higher temperatures with an applied field as small as 0.25 kOe, so they are likely associated with ferromagnetic interactions. We indicate these peaks on the phase diagram with closed square symbols and suggest a phase line with a dotted line connecting these symbols with the open square symbol identifying the position of the $x=0$ shoulder.

The next set of features we identify consist of the low-temperature shoulders and peaks below which χ'_{AC} falls sharply. For $x=0.2$, a low temperature shoulder is evident below the peak. This shoulder in $\chi'_{AC}(x=0.2)$ is effectively field independent for small applied field, and is accompanied by a small peak in χ''_{AC} . χ'_{AC} for both $x=0.3$ and $x=0.4$ exhibits only a single low-temperature peak, below which the susceptibility falls sharply. The susceptibility at temperatures below these peaks is field independent for small applied fields. For $x=0.5$ and $x=0.6$ both a peak and a shoulder are again apparent, shown in more detail in Fig. 9. These low-temperature shoulders are also effectively field independent. A peak is also observed in χ'_{AC} at the shoulder in χ'_{AC} for $x=0.6$. We identify the shoulders in χ'_{AC} for $x=0.2$, $x=0.5$, and $x=0.6$, and the peaks for $x=0.3$ and $x=0.4$, as the signature of a single phase transition, and indicate these features in the phase diagram with diamonds, connected by a dotted line.

Last, we address the peaks found in χ'_{AC} for $x=0.5$ and $x=0.6$. For these two concentrations, the peak moves up in temperature with x , which suggests that they are due to interactions which are distinct from those giving rise to the peaks observed for $x=0.1$ and $x=0.2$. The peaks for $x=0.5$ and $x=0.6$ are suppressed with small applied field. We identify these two peaks with closed triangles, and connect them with a dotted line. These identifications distinguish three low-temperature phases in the phase diagram of Fig. 7. Further work is necessary in order to determine the nature of these phases.

D. $\text{Sr}_3\text{CuPt}_{0.5}\text{Ir}_{0.5}\text{O}_6$

The RQS theory predicts that for half ferromagnetic interactions and half antiferromagnetic interactions along a chain, the susceptibility should be Curie like down to zero temperatures (ignoring any possibility of three-dimensional coupling). Initial dc susceptibility measurements of $\text{Sr}_3\text{CuPt}_{0.5}\text{Ir}_{0.5}\text{O}_6$ at a field of 5 kOe were in qualitative agreement with the theory. Our ac susceptibility measurements, however, are not. Based on our understanding of the three-dimensional ordering in the parent compound, $\text{Sr}_3\text{CuIrO}_6$, it is not surprising that $\text{Sr}_3\text{CuPt}_{0.5}\text{Ir}_{0.5}\text{O}_6$ does not follow the RQS theory. However, we do expect the material to become less three-dimensional and more one-dimensional with increasing Pt concentration as the material becomes more like the one-dimensional Heisenberg antiferromagnet $\text{Sr}_3\text{CuPtO}_6$.

Although we can identify the shoulder in the ac susceptibility of $\text{Sr}_3\text{CuPt}_{0.5}\text{Ir}_{0.5}\text{O}_6$ found near 20 K as a remnant of the three-dimensional ferromagnetic interactions, the origins of the peak and the sharp drop in the susceptibility near 2 K are less clear. The peak height in zero applied field has a small frequency dependence, shown in Fig. 9, but the position of the peak remains essentially constant. This behavior is not consistent with spin-glass behavior. Although spin-glass behavior is expected in three-dimensional systems with competing ferromagnetic and antiferromagnetic interactions,¹⁹ such a phase could be suppressed in this system because of reduced dimensionality. Furthermore, the susceptibility at the lowest temperatures is frequency independent, indicating that the low-temperature state is not frustrated. As is shown in Fig. 8(b) the position of the peak moves towards zero with applied field. This evolution is consistent with antiferromagnetic coupling. The peak is completely suppressed for a field between 2 and 3 kOe.

The sharp drop in the susceptibility at the lowest temperatures is reminiscent of gapped behavior. However, gapped materials are expected to show an increase in the susceptibility as a function of magnetic field, as the field suppresses the gap.²⁰ The field dependence of the susceptibility in $\text{Sr}_3\text{CuPt}_{0.5}\text{Ir}_{0.5}\text{O}_6$ at temperatures below the peak is shown in Fig. 10. It shows that the susceptibility never increases with increased applied field. Instead, the susceptibility is uniformly suppressed, just as it is for the ferromagnetic compound $\text{Sr}_3\text{CuIrO}_6$. It is still possible that a peak due to the suppression of the gap could be hidden since we may be measuring the transverse susceptibility along with the longitudinal susceptibility in the powder sample.

IV. DISCUSSION

We have found that the solid solution $\text{Sr}_3\text{CuPt}_x\text{Ir}_{1-x}\text{O}_6$ does not behave according to the RQS theory, primarily be-

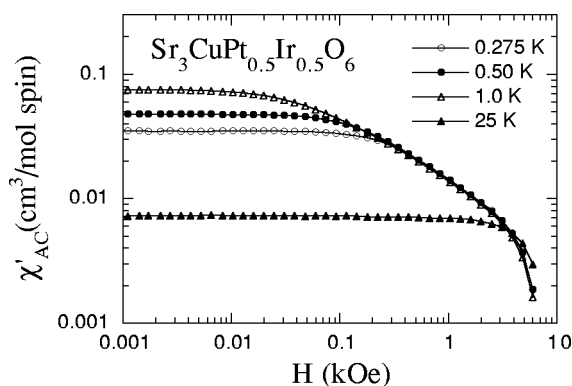


FIG. 10. Log χ'_{AC} vs log applied field at temperatures below the peak in χ'_{AC} vs temperature ($T=0.275, 0.5,$ and 1.0 K). χ'_{AC} is shown in the paramagnetic region at $T=25$ K for comparison.

cause of three-dimensional ferromagnetic correlations between the chains of magnetic ions. In order to gain a deeper understanding of the behavior of the series of materials, we consider theories which have been developed to address disorder in three-dimensional materials.

Percolation theory has been used to describe the behavior of ferromagnets diluted with nonmagnetic ions.²¹ As nonmagnetic ions replace ferromagnetic ions, percolation theory predicts that the ferromagnetic transition temperature will be suppressed. The concentration of magnetic ions p reaches a percolation concentration p_c in the limit that a path of magnetic bonds extends across the whole sample. The ferromagnetic transition disappears at the percolation concentration, but for all magnetic concentrations above the percolation concentration, the susceptibility is predicted to exhibit a sharp peak at the transition temperature $T_c(p)$. The critical percolation concentration (p_c), as well as the functional form of $T_c(p)$, depends on lattice dimensionality and the range of interaction. A number of diluted ferromagnets have been found to follow percolation theory.²¹

Percolation theory has been extended to include mixed

ferromagnetic and antiferromagnetic systems, where a similar depression in $T_c(p)$ is predicted.²² Furthermore, a linear suppression of the ferromagnetic transition temperature and a percolation concentration of 0.41 was observed in the two-dimensional disordered ferromagnet with competing antiferromagnetic interactions, $\text{Rb}_2\text{Mn}_x\text{Cr}_{1-x}\text{Cl}_4$, as is expected from percolation theory.²³ However, in $\text{Sr}_3\text{CuPt}_x\text{Ir}_{1-x}\text{O}_6$ the ferromagnetic phase line does not decrease with x as rapidly as percolation theory predicts. In addition, the peak in the susceptibility is rapidly suppressed to a shoulder, unlike the behavior exhibited in a ferromagnet diluted with nonmagnetic ions. Although the paramagnetic susceptibility indicates that the magnetic ions are well mixed in the samples, it is impossible to rule out the existence of a small number of crystallites of the pure ferromagnetic phase. Furthermore, there are likely to exist statistically rare regions (“Griffiths phase”) of pure ferromagnetic correlations, which may also contribute to the powder susceptibility.²⁴

There are many complicated issues to consider in understanding the behavior of this system. The details of the magnetic structures of $\text{Sr}_3\text{CuIrO}_6$ and $\text{Sr}_3\text{CuPtO}_6$ are not even known. The nature of the low-temperature phases of all of the samples is unclear. More experimental techniques need to be applied to these materials in order to determine the nature of both the ordered systems and the disordered systems in the solid solution series. Furthermore, large single crystals would help to clarify the magnetic structure in these materials. What is clear about the $\text{Sr}_3\text{CuPt}_x\text{Ir}_{1-x}\text{O}_6$ system is that it is more complicated and rich than previous experiments indicated, and that the RQS theory cannot be applied to it in a straightforward way.

ACKNOWLEDGMENTS

The work at Wesleyan University was supported by NSF Grant No. DMR-97-33848. The work at the University of South Carolina was supported by NSF Grant No. DMR-98-73570.

¹M. Steiner, J. Villain, and C. Windsor, *Adv. Phys.* **25**, 87 (1976).

²E. Fradkin, *Field Theories of Condensed Matter Systems* (Addison-Wesley, Redwood City, CA, 1991).

³A. P. Wilkinson, A. K. Cheetham, W. Kunman, and A. Kvick, *Eur. J. Solid State Inorg. Chem.* **28**, 453 (1991).

⁴T. N. Nguyen and H.-C. zur Loye, *J. Solid State Chem.* **117**, 300 (1995).

⁵P. Nunez, S. Trail, and H.-C. zur Loye, *J. Solid State Chem.* **130**, 35 (1997).

⁶H. Kageyama, K. Yoshimura, K. Kosuge, H. Mitamura, and T. Goto, *J. Phys. Soc. Jpn.* **66**, 1607 (1997).

⁷O. C. Lampe, M. Sigrist, and H.-C. zur Loye, *J. Solid State Chem.* **127**, 25 (1996).

⁸J. Claridge, R. Layland, W. Henley, and H.-C. zur Loye, *Chem. Mater.* **11**, 1376 (1999).

⁹T. N. Nguyen, P. A. Lee, and H.-C. zur Loye, *Science* **271**, 489 (1996).

¹⁰A. Furusaki, M. Sigrist, P. A. Lee, K. Tanaka, and N. Nagaosa, *Phys. Rev. Lett.* **73**, 2622 (1994).

¹¹A. Furusaki, M. Sigrist, E. Westerberg, P. A. Lee, K. B. Tanaka, and N. Nagaosa, *Phys. Rev. B* **52**, 15 930 (1995).

¹²E. Westerberg, A. Furusaki, M. Sigrist, and P. A. Lee, *Phys. Rev. B* **55**, 12 578 (1997).

¹³B. Ammon and M. Sigrist, *J. Phys. Soc. Jpn.* **68**, 1018 (1999).

¹⁴B. Frischmuth, M. Sigrist, B. Ammon, and M. Troyer, *Phys. Rev. B* **60**, 3388 (1999).

¹⁵T. N. Nguyen, D. Giaquinta, and H.-C. zur Loye, *Chem. Mater.* **6**, 1644 (1994).

¹⁶T. Arioka, H. Ohta, S. Okubo, R. Kanno, and N. Kitamura, *J. Magn. Magn. Mater.* **177-181**, 653 (1988).

¹⁷J. M. Yeomans, *Statistical Mechanics of Phase Transitions* (Oxford, London, 1992).

¹⁸S. Chikazumi and S. H. Charap, *Physics of Magnetism* (Wiley, New York, 1959).

¹⁹A. K. Hartmann, *Phys. Rev. B* **59**, 3617 (1999).

²⁰M. Chitra and T. Giamarchi, *Phys. Rev. B* **55**, 5816 (1997).

²¹C. Domb and J. Lebowitz, *Phase Transitions and Critical Phenomena* (Academic, London, 1983), Vol. 7, p. 152.

²²J. Jakubczak, Z. Mrozińska, and A. Pekalski, *J. Phys. C* **12**, 2341 (1979).

²³G. Münnighoff, W. Kurtz, W. Treutmann, E. Hellner, G. Heger, N. Lehner, and D. Reinen, *Solid State Commun.* **40**, 571 (1981).

²⁴H. Rieger, *Physica A* **266**, 471 (1999).